Three-dimensional, Multi-Phase Unsteady Flow of Water Undergoing Multiple Flow Regimes (free surface, droplet, and fluid film)

William M. Dziedzic
NASA Kennedy Space Center, FL 32899

Abstract

Upgrades to the Mobile Launcher Rainbird nozzles were implemented for the Artemis II launch to increase water flow rates and improve the mobile launcher deck water coverage while minimizing the water throw distance to avoid impacting the Space Launch System (SLS) rocket nozzles. This analysis describes the use of a three-dimensional, multi-phase, free surface transient computational fluid dynamics (CFD) model to simulate the water flowing out through the Rainbird nozzle and ensure compliance with current Artemis requirements. Flow rates, pressures, velocities, nozzle throw distances and coverage areas were analyzed to ensure that system requirements are met. The completed results were used to make necessary modifications to the Ignition Overpressure Protection and Sound Suppression (IOP/SS) system Rainbird design by reshaping the nozzle used in the system.

Introduction

At launch, the SLS rocket produces nearly nine million pounds of thrust, generating sound waves that, if not mitigated, would reflect off the pad and Mobile Launcher, shaking the rocket violently and potentially causing it to tear itself apart. NASA's Ignition Overpressure Protection and Sound Suppression (IOP/SS) system uses a water deluge to help dampen the extreme acoustic energy, heat, and vibration produced at liftoff to keep the rocket and launch pad safe. During the launch of Artemis, 450,000 gallons of water will be released onto the mobile launcher and flame deflector, with a peak flowrate of 1.1 million gallons per minute.

Figure 1 Artemis II Launch on April 1, 2026[1]

Figure 2 Water Suppression System[2]

Figure 3 Water Suppression System (Partial Flow)[3]

Figure 4 Water Suppression System (Full Flow)

The objective of the analysis was to ensure that the nozzle shapes provided adequate coverage across the blast deck between the north and south Rainbirds. Another objective of the analysis was to examine the interaction of the Northwest Rainbird and the North Center Rainbird. It was expected that the water from the nozzles would flow between the two North Rainbirds and interact with one another. This interaction could potentially lead to vehicle impingement. The CFD simulation was able to provide the flow rate of water and droplet size of the water, to determine whether there were large droplets or a mist in the vehicle area. The analysis was later verified by Verification and Validation (V&V) testing at the pad.

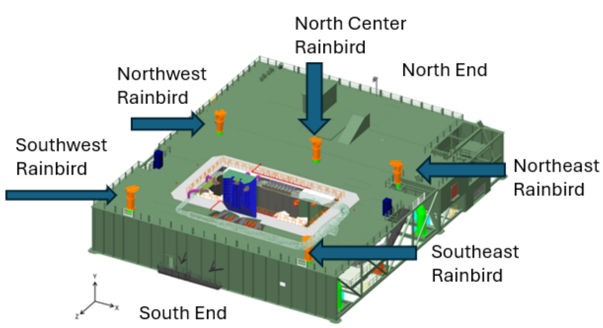

Figure 5 KSC Pad 39 B Mobile Launch Base showing Rainbirds

Modeling

This CFD study involves three dimensional, implicit unsteady, Lagrangian multiphase, hybrid multiphase (air and water), Multiphase interactions, gravity, fluid film, and segregated flow. The term hybrid multiphase refers to modeling multiple flow regimes of a phase material using a combination of several different multiphase models. In a hybrid multiphase simulation, each multiphase model covers a particular flow regime. The transition of a phase material between flow regimes is handled through phase interactions taking into account local flow conditions and mesh cell size.

Initially, the entire computation domain is filled with the continuous air phase. To simulate the flow of two materials: air and water, the water transitions to different flow regimes, each of which is modeled by a different multiphase model, this requires a water phase for each multiphase model type. The air phase remains continuous and is modeled by the VOF model only.

The multiphase segregated flow model treats each phase as inter-penetrating continua. It solves transport equations for mass, momentum, and energy of each phase while all the phases share a common pressure field. Eulerian averaging of the transport equations results in additional interaction between the phases.

The water exits the Rainbird nozzle, thus forming a large-scale interface between water and air. Primary break-up of the jet creates large contiguous water droplets and ligaments. Both flow regimes are modeled using the Volume of Fluid (VOF) model. Free surface water jet with large, resolved droplets and ligaments. The VOF method has an Eulerian air phase and Eulerian water phase.

The large water droplets and ligaments (also known as VOF blobs) break up into smaller water droplets. When the diameter of small spherical water droplets falls below a certain threshold, they transition to Lagrangian droplets whose paths are tracked using the Lagrangian Multiphase model. The VOF to Lagrangian conversion is handled by the Resolved Eulerian-Lagrangian Transition phase interaction model. When the Lagrangian water droplets and VOF blobs impinge on the floor, they form thin film puddles that can accumulate to a pool of water. The thin water film is modeled either in an unresolved way by the Fluid Film model or in a resolved way by the VOF model. Based on volume fraction and cell size, the Resolved Fluid Film phase interaction model determines which approach is taken.

The shape and position of the interface between water and air is influenced by surface tension effects. The surface tension force for all phase interactions describes the relation between water and air.

Adaptive mesh refinement (AMR) is employed to locally refine the mesh along the water-air free surface. Once a VOF blob has transitioned to a Lagrangian droplet, AMR coarsens the mesh.

Adaptive meshing refines the mesh locally along the interface between air and water when these two phases form a free surface or VOF blobs under the control of the VOF model. A phase interface is detected over a maximum of 10 cells, and cells that fulfill the refinement criterion can be refined up to four times. The time-step uses the Free Surface CFL Condition, which sets the time-step based on the convective Courant number (CFL number) weighted by the rate of change of volume fraction.

Each mesh type is shown in Figure 6.

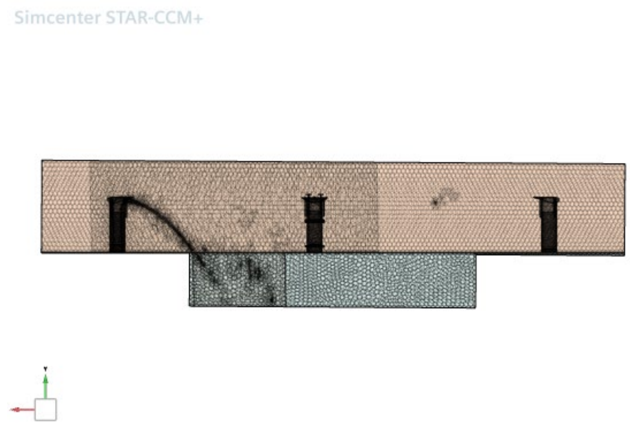

Figure 6 Mesh with adaptive mesh

General Equations

The Eulerian Mixture Multiphase models fluid phases by solving transport equations for mass, momentum, and energy for the mixture of phases rather than for each phase separately. To calculate the distribution of phases, the volume fraction transport equation is solved for each phase. For phases that are moving at different velocities, algebraic relations are used to compute the relative velocities. In STAR-CCM+, this approach is called N-Phase Mixture model.[4]

Volume Fraction

The share of the flow domain that is occupied by each phase is given by its volume fraction.
The volume of a phase is given by:

$$V_i = \int_V \alpha_i dV \tag{1}$$

where α_i is the volume fraction of phase i.

The volume fractions of each Eulerian phase must fulfill the requirement:

$$\sum_{i=1}^{n} \alpha_i = 1 \tag{2}$$

Where n is the number of all phases.

Continuity Equation

The conservation of mass for a generic phase i is given by:

$$\frac{\partial}{\partial t}\int_V \alpha_i \rho_i dV + \oint_A \alpha_i \rho_i v_i \cdot da = \int_V \sum_{j \neq i} \left(m_{ij} - m_{ji} \right) dV + \int_V S_i^{\alpha} dV \tag{3}$$

where:

- α_i is the volume fraction
- ρ_i is the density
- v_i is the velocity
- $m_{ij}$is the mass transfer rate to phase i, from phase j ($m_{ij} \geq 0$)
- m_{ji} is the mass transfer rate to phase j, from phase i ($m_{ji} \geq 0$)
- S_i^α is a user-defined phase mass source term

Momentum Equation

The momentum balance for the generic phase i read:

The volume fractions are transported according to the following conservation equation:

$$\frac{\partial}{\partial t}\int_V \alpha_i \rho_i v_i \, dV + \oint_A \rho_i v_i \otimes v_i \otimes v_i \cdot da = -\int_V \alpha_i \nabla p dV$$

$$+ \int_V \alpha_i \rho_i g dV + \oint_A \left[\alpha_i\left(T_i + T_i^t\right)\right] \cdot da + \int_V M_i dV$$

$$+ \int_V (F_{int})_i dV + \int_V S_i^\alpha dV + \int_V \sum_{i=1}^n \left(m_{ij} v_j - m_{ji} v_i\right) dV \tag{4}$$

where:

- p is the pressure, assumed to be equal in all phases
- g is the gravity vector
- T_i and T_i^t are the molecular and turbulent stresses, respectively
- M_i is the interphase momentum transfer per unit volume
- $(F_{int})_i$represents internal forces (such as the solid pressure force between particles or a user-defined potential force)
- S_i^α is the phase momentum source term
- m_{ij} is the mass transfer rate from phase j to phase i.
- m_{ji} is the mass transfer rate from phase i to phase j.

The interphase momentum transfer represents the sum of all the forces the phases exert on one another and satisfies the equation:

$$\sum_i M_i = 0 \tag{5}$$

Energy Equation

Energy is conserved for a Eulerian phase according to the following equation:

$$\frac{\partial}{\partial t}\int_V \alpha_i \, \rho_i E_i dV + \oint_A \alpha_i \rho_i H_i v_i \cdot da = \oint_A \alpha_i k_{eff,i} \nabla T_i da + \oint_A T_i \cdot v_i da$$

$$+\int_V f_i \cdot v_i dV + \int_V \sum_{j\neq i} Q_{ij} dV + \int_V \sum_{ij} Q_i^{(ij)} dV + \int_V S_{u,i} dV + \int_V \sum_{j\neq i} (m_{ij} - m_{ji}) h_i\,(T_{ij}) dV\, dV$$

$$+\int_V \sum_{j\neq i} (m_{ij} - m_{ji}) h_i\,(T_{ij}) dV\, dV \quad (6)$$

where:

- E_i is the total energy.
- H_i is the total enthalpy.
- T_i is the viscous stress tensor.
- α_i, ρ_i, and v_i are the volume fraction, density, and velocity of phase i.
- T_i is the temperature.
- $k_{eff,i}$ is the effective thermal conductivity.
- f_i is the body force vector.
- Q_{ij} is the interphase heat transfer rate to phase i from phase j. It refers to heat transfer between phases due to a temperature difference between the phases.
- $Q_i^{(ij)}$ is the heat transfer rate to phase i from phase pair interface (ij). It refers to the heat transfer phenomena such as evaporation, condensation, and boiling where heat transfer occurs between the phase and the interface.
- $S_{u,i}$ is the energy source.
- $h_i(T_{ij})$ is the phase i enthalpy that is evaluated at the interface temperature T_{ij}.

The effective thermal conductivity $k_{eff} is$:

$$k_{eff,i} = k_i + \frac{\mu_{t,i} C_{p,i}}{\sigma_{t,i}} \quad (7)$$

where:

- $k_i$is the thermal conductivity.
- $\mu_{t,i}$ is the turbulent viscosity.
- $C_{p,i}$ is the specific heat.
- $\sigma_{t,i}$ is the turbulent thermal diffusion Prandtl number.

Total energy, E, is related to total enthalpy, H, by

$$E_i = H_i - \frac{p}{\rho_i} \quad (8)$$

Where:

$$H_i = h_i + \frac{|v_i|^2}{2} \quad (9)$$

and

$$h_i(T_i) = h_i^{REF} + \int_{T_i^{REF}}^{T_i} C_{p,i}\,(T')\, dT' \quad (10)$$

where $h_i^{REF}$is the heat of formation for phase i and T_i^{REF} is the standard state temperature for phase i.

When heat is transferred only by thermal diffusion between phases, the interphase heat transfer rates satisfy $Q_{ij} = -Q_{ji}$. Where heat and mass are only transferred by phase change (bulk boiling or condensation), the heat transfer rates between each phase i, j, and a phase pair interface (ij) satisfy a heat balance:

$$Q_i^{(ij)} + Q_j^{(ij)} + (m_{ij} - m_{ji})\Delta h_{ij} = 0 \quad (11)$$

where Δh_{ij} is the heat required to produce phase i from phase j. This is a signed quantity so that $\Delta h_{ij} = -\Delta h_{ji}$. The heat of phase change is defined from the phase enthalpy definitions that are evaluated at the interface temperature T_{ij}:

$$\Delta h_{ij} = h_j(T_{ij}) - h_i(T_{ij}) \quad (12)$$

Analysis Results

The figures below show a series of volume fraction of water iso-surface plots of the water as it exits the nozzle. The particle diameter and water film thickness is also included. Eventually the water reaches the deck and forms a pool across the deck floor with varying thickness towards the flame trench.

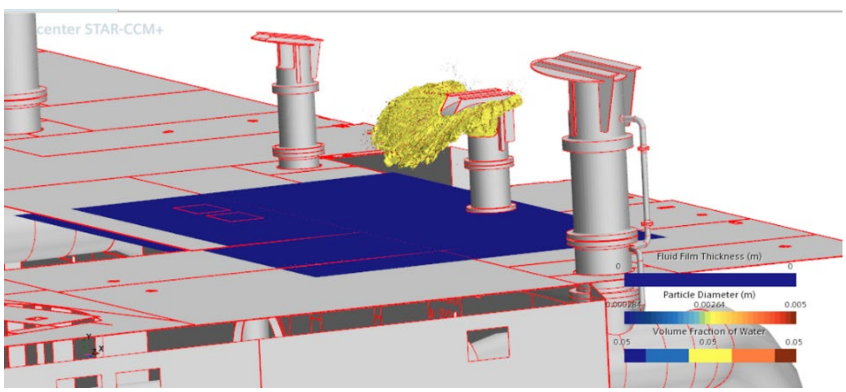

Figure 7 Iso-surface plot Volume Fraction of Water, Particle Diameter (m), Water Film Thickness (m)

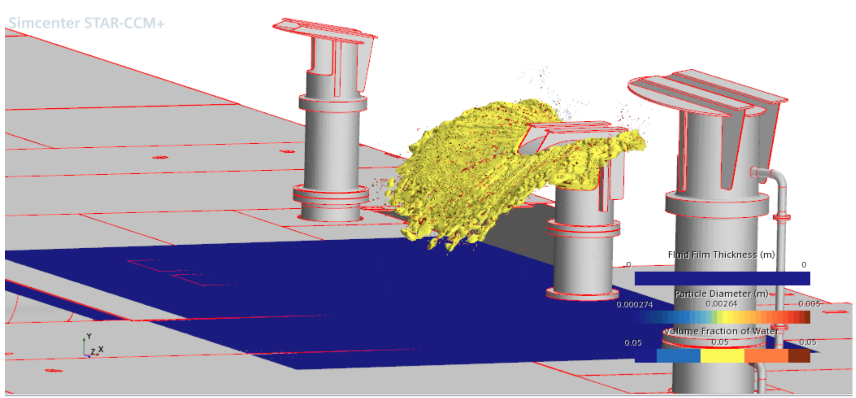

Figure 8 Iso-surface plot Volume Fraction of Water, Particle Diameter (m), Water Film Thickness (m)

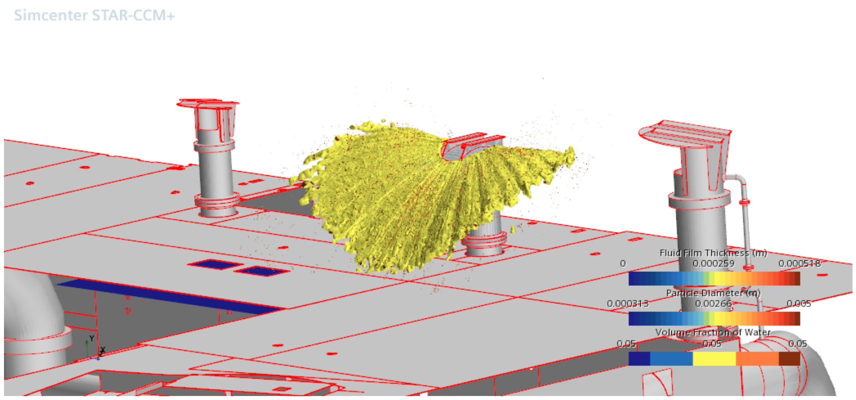

Figure 9 Iso-surface plot Volume Fraction of Water, Particle Diameter (m), Water Film Thickness (m)

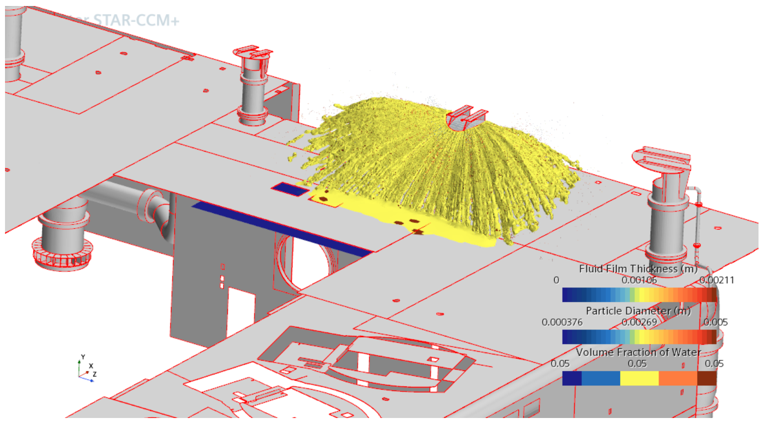

Figure 10 Iso-surface plot Volume Fraction of Water, Particle Diameter (m), Water Film Thickness (m)

A pressure contour plot within the nozzle is shown in the figure below.

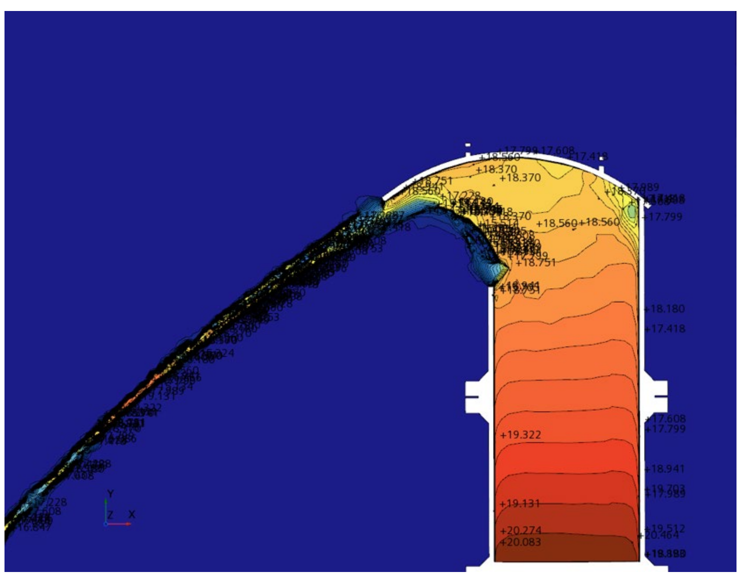

Figure 11 Pressure Contour Plot

A velocity contour plot within the nozzle is shown in Figure 12.

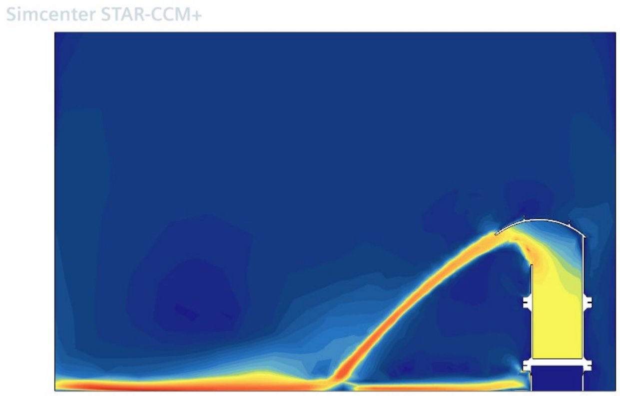

Figure 12 Velocity Contour Plot

Velocity vector plots for three of the nozzles are shown below.

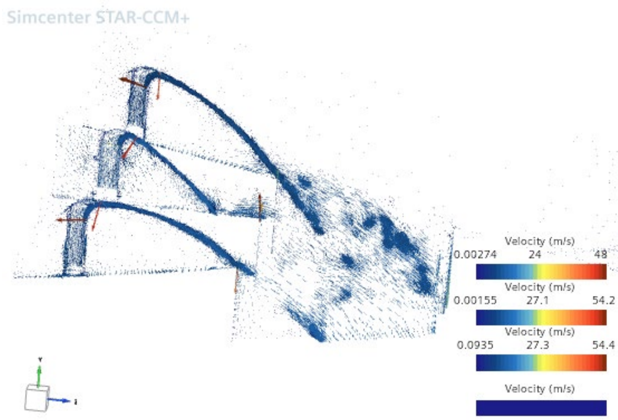

Figure 13 Velocity Vector Plot across Three Nozzles

A top view for the volume fraction of water iso-surface plot is shown from three of the nozzles showing the throw distance of the water, the particle diameter and film thickness across the deck.

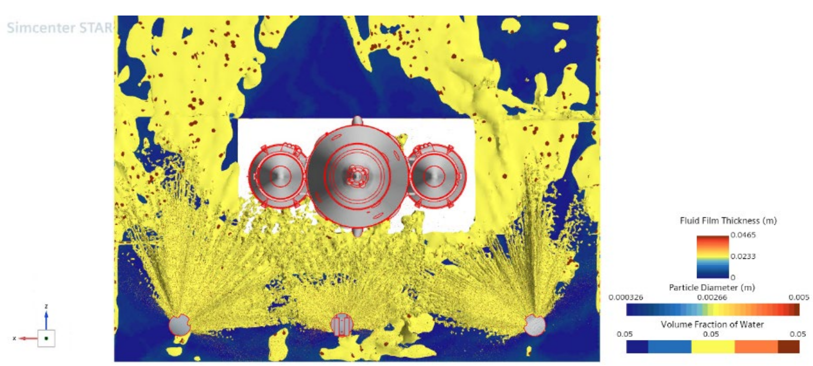

Figure 14 Top View Three Nozzles Iso-surface plot showing Volume Fraction of Water, Particle Diameter (m), Water Film Thickness (m)

A perspective view for the volume fraction of water iso-surface plot is shown from three of the nozzles showing the throw distance of the water, the particle diameter and film thickness across the deck.

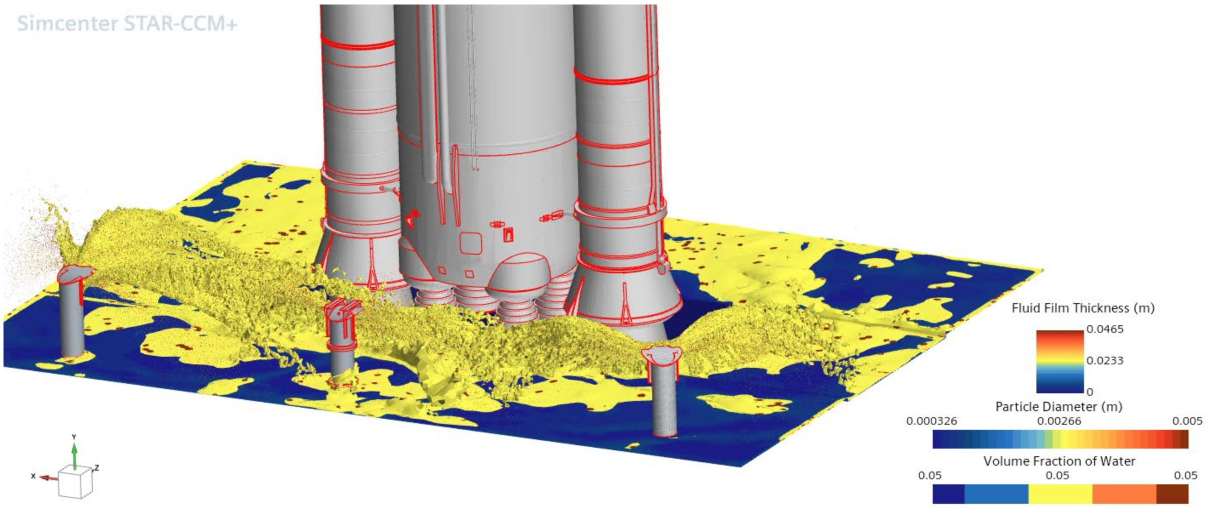

Figure 15 Perspective View Three Nozzles Iso-surface plot showing Volume Fraction of Water, Particle Diameter (m), Water Film Thickness (m)

The figure below shows a top view of all five nozzle iso-surface plot showing the Volume of Fraction of Water, Particle, Diameter, and Water Film Thickness.

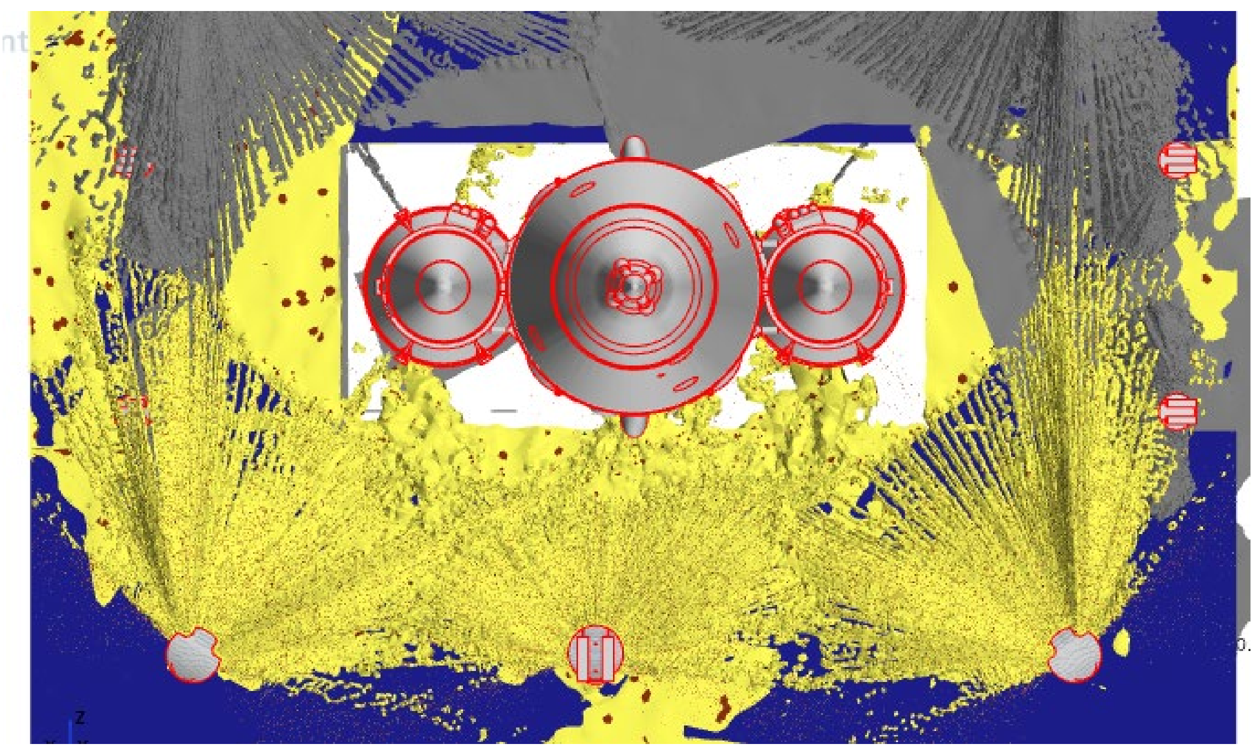

Figure 16 Top View All Five Nozzles Iso-surface plot showing Volume Fraction of Water, Particle Diameter (m), Water Film Thickness (m)

Conclusion

The CFD simulation results indicated that the modified Rainbirds would provide adequate coverage between the north and south Rainbirds and along the sides of the blasthole. Also, CFD analysis predicted that the deflection of water caused by the curved nozzle would allow the water to fall short of the vehicle at full flow, thus mitigating the vehicle impingement. It was expected that the water from the nozzles would flow between the two North Rainbirds and interact with one another. The CFD simulation was able to provide the flow rate and droplet size of the water, i.e., large droplets or mist in the vehicle area. The CFD simulation results compared well with the V&V test results and showed that the interaction of water between the nozzles is in the form of a mist and not a direct impingement on the SLS vehicle.

References

1. *https://www.nasa.gov/image-detail/artemis-ii-launch-3/*
2. *https://www.nasa.gov/centers-and-facilities/kennedy/pad-39b-water-flow-test-comes-through-loud-and-clear/*
3. https://www.youtube.com/watch?v=mn7WMowM1xY&vl=en
4. CD-adapco, 2019. Star-CCM+ User Guide. (Eulerian Multiphase (EMP) Flow)